J. Membrane Biol. 119, 229–239 (1991)
002226319100022H

The Journal of
Membrane Biology

Inactivation Kinetics and Pharmacology Distinguish Two Calcium Currents in Mouse Pancreatic B-Cells

William F. Hopkins, Leslie S. Satin, and Daniel L. Cook
Departments of Physiology and Biophysics, and Medicine, University of Washington School of Medicine, Seattle, Washington, and Division of Metabolism, Seattle Veterans Administration Medical Center (151), Seattle, Washington 98108

Summary. Voltage-dependent calcium currents were studied in cultured adult mouse pancreatic B-cells using the whole-cell voltage-clamp technique. When calcium currents were elicited with 10-sec depolarizing command pulses, the time course of inactivation was well fit by the sum of two exponentials. The more rapidly-inactivating component had a time constant of 75 ± 5 msec at 0 mV and displayed both calcium influx- and voltage-dependent inactivation, while the more slowly-inactivating component had a time constant of 2750 ± 280 msec at 0 mV and inactivated primarily via voltage. The fast component was subject to greater steady-state inactivation at holding potentials between −100 and −40 mV and activated at a lower voltage threshold. This component was also significantly reduced by nimodipine (0.5 μM) when a holding potential of −100 mV was used, whereas the slow component was unaffected. In contrast, the slow component was greatly increased by replacing external calcium with barium, while the fast component was unchanged. Cadmium (1–10 μM) displayed a voltage-dependent block of calcium currents consistent with a greater effect on the high-threshold, more-slowly inactivating component. Taken together, the data suggest that cultured mouse B-cells, as with other insulin-secreting cells we have studied, possess at least two distinct calcium currents. The physiological significance of two calcium currents having distinct kinetic and steady-state inactivation characteristics for B-cell burst firing and insulin secretion is discussed.

Key Words calcium currents · pancreatic B-cells · inactivation

Introduction

In response to suprathreshold (>7 mM) glucose stimulation, pancreatic B-cells depolarize and undergo periodic plateau depolarizations upon which are superimposed action potentials (Dean & Matthews, 1970*a*; Meissner & Schmelz, 1974). Both the plateau depolarizations and action potentials are calcium-dependent (Dean & Matthews, 1970*b*; Ribalet & Beigelman, 1980; Meissner & Schmeer, 1981), and the calcium uptake associated with these events triggers insulin secretion (Wollheim & Sharp, 1981; Wollheim & Pozzan,1984). Voltage-dependent calcium currents, which underly these events, were first described in neonatal rat B-cells (Satin & Cook, 1985) and insulin-secreting RINm5F cells (Findlay & Dunne, 1985) using the whole-cell patch-clamp technique. Subsequent work using these preparations (neonatal rat: Satin & Cook, 1988; RINm5F: Velasco, 1987; Velasco, Petersen & Petersen, 1988), insulin-secreting HIT cells (Satin & Cook, 1988, 1989; Keahy et al., 1989), and cultured adult rat (Hiriart & Matteson, 1988) and mouse B-cells (Rorsman & Trube, 1986; Rorsman, Ashcroft & Trube, 1988; Plant, 1988*b*) have further characterized some of the properties of calcium currents and channels in these cells.

We have presented a variety of evidence that neonatal rat and HIT cells possess at least two kinetically distinct components of voltage-dependent calcium current (Satin & Cook, 1988, 1989). Here we present evidence for two calcium current components in mouse B-cells with distinct kinetic and steady-state inactivation properties. These fast and slow current components can also be distinguished on the basis of their activation thresholds, sensitivity to calcium channel antagonists (nimodipine and cadmium) and divalent cation selectivity. Taken together, the data suggest that cultured adult mouse B-cells, like neonatal rat and HIT cells, possess at least two types of calcium currents.

A preliminary account of this work has appeared (Hopkins, Satin & Cook, 1989).

Materials and Methods

Cell Culturing

Islets were isolated from the pancreases of adult female Swiss-Webster mice using collagenase digestion. Single islet cells were mechanically dispersed from islets in a zero calcium buffer and

subsequently plated on polylysine-coated glass cover slips. All data were obtained using cells cultured for one week or less, although calcium currents could be recorded from cells kept in culture for up to four weeks. Immunostaining for insulin (Baskin, Gorray & Fujimoto, 1984) demonstrated that greater than eighty per cent of cells cultured in this manner were B-cells (Satin et al., 1989).

Patch-Clamp Techniques

Single cells were observed by using an inverted microscope and whole-cell voltage clamped (Hamill et al., 1981) at room temperature (20–22°C) by using a Dagan 8900 patch-clamp amplifier (Dagan, Minneapolis, MN) and fire-polished soda glass pipettes (3–7 MΩ in standard internal solution). Junction potentials were nulled with the pipette in the bathing solution by using an auto search circuit. Series resistance compensation was not routinely used since the inward currents recorded were typically less than 200 pA in amplitude. Voltage pulse protocols were produced with a microcomputer (TRS-80; Tandy, Fort Worth, TX). Such pulses were used to elicit calcium currents and determine current-voltage relations (*I-V*'s, 40 msec pulses delivered at 0.2 Hz), as previously described (Satin & Cook, 1988).

Data were recorded on VCR tape using a PCM data recorder (Neurocorder DR-866; Neuro Data, New York) and digitized both off- and on-line by a microcomputer data acquisition system (Metaresearch, Portland, OR; Macintosh SE; Apple Computer, Cupertino, CA) and current responses to 10 sec voltage pulses were digitized at 1–10 kHz by another data acquisition system (MacADIOS II, GW Instruments, Cambridge, MA). Current traces were digitized at 10 kHz for the first 100 msec and the remainder at 1 kHz. Data were filtered at 1 kHz by an 8-pole Bessel filter (Frequency Devices, Haverhill, MA) prior to digitization. The linear leakage conductance about the holding potential was determined by the method of least squares, and extrapolated leak current values were subtracted from the current elicited by each corresponding voltage pulse. Leak-subtracted *I-V*'s were determined in this manner. However, individual current traces shown in the figures are not leak- or capacity-current subtracted. Some cells displayed an outward "nonlinear leak" current at potentials more positive than 0 mV, which we observed in neonatal rat and HIT cells (Satin & Cook, 1988, 1989) and has also been observed in cultured mouse B-cells (Plant, 1988*b*). When present, this current manifested itself as a progressive leftward shift in the apparent calcium current reversal potential during the course of a recording. The ionic nature of this current is unknown (but *see* Satin & Cook, 1989).

A nonlinear curve-fitting algorithm (Igor software, Wavemetrics, Lake Oswego, OR) was used to fit the time course of current inactivation as the sum of exponential terms plus a constant, asymptotic current level. If the chi-square value of the best fit yielded a *p*-value greater than 0.05, the fit and data were rejected. Data were also rejected if the current relaxed beyond the estimated linear leak current level. Of 18 cells, 14 were fit by this criterion and are presented in this paper. However, all four cells not fit by two exponentials were adequately fit by the sum of three exponential terms. Five of the 14 acceptable cells were also adequately fit by the sum of three exponentials. None of the data were well fit with a single exponential function. The function yielded coefficients (current amplitudes) and rate constants (reciprocal time constants) for each current component. All values are expressed as mean ± SEM, and differences between means were evaluated statistically with the *t*-test or the Mann-Whitney U-test. The statistical significance level was chosen as $p < 0.05$.

Solutions and Drugs

External solutions had the following composition (in mM): 120 NaCl, 20 tetraethylammonium (TEA), 5 CsCl, 3 $CaCl_2$, 1 $MgCl_2$, 0.0005 tetrodotoxin (TTX), 11.1 glucose, 10 HEPES, pH = 7.2. In some experiments, 3 or 10 mM barium replaced 3 or 10 mM calcium, respectively. Cadmium (1–10 μM) was directly dissolved in the external saline in experiments requiring it. The pipette solution contained (in mM): 114 CsAspartate, 10 CsCl, 10 4-aminopyridine (4-AP), 2 $MgCl_2$, 2 ATP, 1 EGTA, 20 HEPES, pH = 7.2; pH was adjusted with CsOH. TTX was included to block inward sodium currents (Plant, 1988*a*), cesium, TEA and 4-AP were used to block voltage- and calcium-dependent outward potassium currents (Hille, 1984; S. Fatherazi and D.L. Cook, *unpublished observations*), and ATP was included to suppress ATP-sensitive potassium current (Cook & Hales, 1984). Assuming 30 μM contaminating calcium in the pipette solution, the free calcium concentration with 1 mM EGTA was calculated to be about 5 nM, while the estimated free EGTA concentration was 0.9 mM (Fabiato & Fabiato, 1979).

Nimodipine (10 mM) was dissolved in dimethyl sulfoxide (DMSO), and microliter aliquots were added to the external solution. The final DMSO concentration was never more than 0.1% (vol/vol). Precautions were taken to shield the nimodipine solutions from light.

Results

Kinetics of Calcium Current Inactivation

When 10 sec depolarizing pulses to 0 mV were applied from a holding potential of −100 mV, calcium currents inactivated with complex kinetics. Figure 1 illustrates the curve-fitting procedure, and the figure legend lists the output parameters obtained for the current trace shown. Table 1 lists mean current amplitudes (coefficients of the exponential terms) and time constants of the two (fast and slow) components. The fast current component (mean time constant = 75 msec) was over 30-fold faster than the slow component (mean time constant = 2750 msec), and represented 36% of the total current on average (at 0 mV). The noninactivating component (corresponding to the constant term in the fitting equation) was 7.7 ± 1.3 pA, which represented 11 ± 2% of the total calcium current. Since all cells possessed comparable fast and slow components, this paper will focus on these components.

Characteristics of Rapidly-Inactivating Component

Inactivation of calcium currents may be due to calcium influx- and/or voltage-dependent mechanisms (for review, *see* Eckert & Chad, 1984). To determine

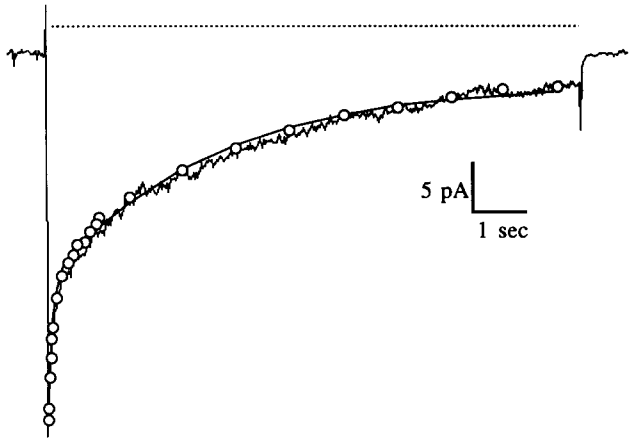

Fig. 1. Calcium current elicited by 10 sec voltage pulse to 0 mV from a holding potential of −100 mV. Current trace is not capacity- or leak-subtracted. The dashed line indicates the linear leak current. The filter setting was 1 kHz. Data were digitized and digitally binned (open circles; 10 msec bins for the first 100 msec; 100 msec bins for the next 900 msec and 1 sec bins for the remaining 9 sec). The binned values were fit with the equation $I(t) = K_0 + K_1 e^{(-K_2 t)} + K_3 e^{(-K_4 t)}$, where I is current (pA), t is time (sec), K_0 is the steady, asymptotic current, K_1 and K_3 are the slow and fast component coefficients, respectively, and K_2 and K_4 are the slow and fast component rate constants, respectively. The values for these parameters for this example are $K_0 = -3.86$ pA, $K_1 = -20.29$ pA, $K_2 = 0.33$ sec^{-1}, $K_3 = -17.65$ pA, $K_4 = 14.42$ sec^{-1}. The fitting equation is indicated by the continuous line. The chi square value for the fit is 8.64 ($n = 27$ points, $P < 0.05$)

Table 1. Time constants and coefficients for two-exponential fits to inactivation time course during 10-sec pulses to 0 mV from holding potential of −100 mV[a]

	Fast component	Slow component
Time constants (msec)	75 ± 5	2750 ± 280
Coefficients (pA)	24.5 ± 3.2	36.3 ± 6.1

[a] Data from 14 cells, 3 mM calcium charge carrier. Values are expressed as mean ± SEM.

the mechanism of the fast component of inactivation, a three-pulse protocol was used with either 3 mM calcium or barium as charge carrier (Fig. 2*A*). In this protocol, the inactivation produced by the middle (or conditioning) 100-msec pulse was quantitated as the % inactivation of the third (test) pulse relative to the first (control) pulse. This protocol controlled for run-down of calcium current amplitude and changes in leakage current (Satin & Cook, 1989). In Fig. 2*B* and *C*, the peak current amplitudes elicited by conditioning pulses to various voltages (conditioning pulse *I-V*) are plotted on the same axis as the inactivation produced by the conditioning

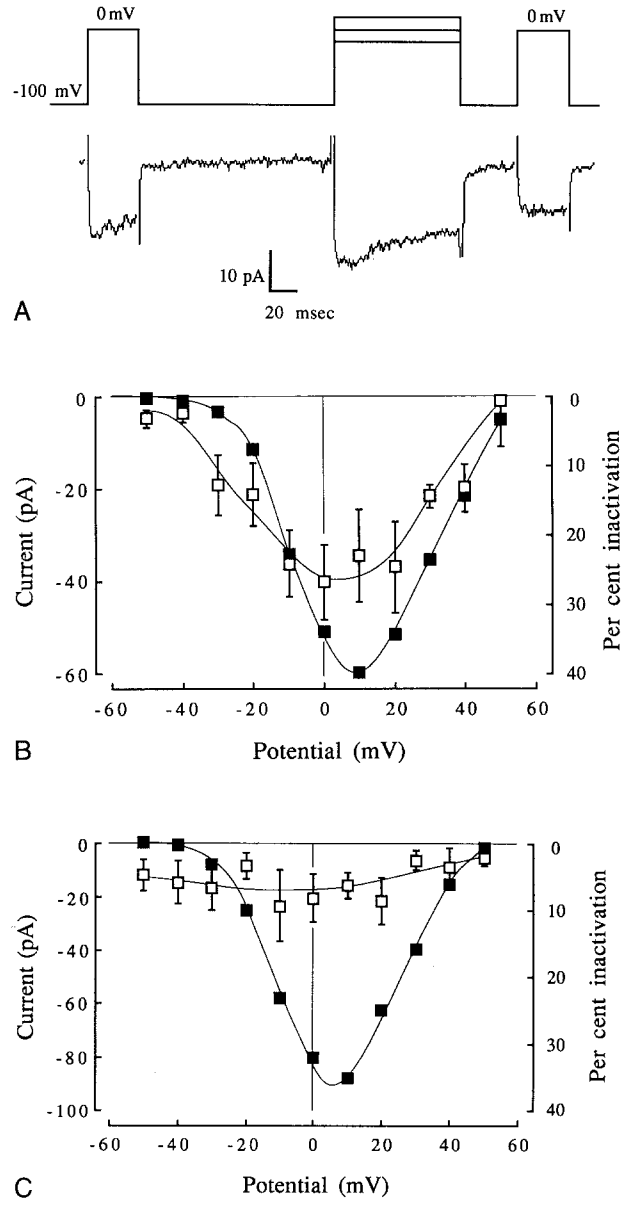

Fig. 2. (*A*) Three-pulse protocol to test for calcium influx-dependent inactivation of calcium current. The control (first) and test (third) voltage pulses were of fixed duration and amplitude (40 msec and 0 mV, respectively, although in some experiments 10-msec pulses were used with similar results), and the conditioning (second) pulse voltage (100 msec duration) was varied in amplitude between −100 and +50 mV. The holding potential was −100 mV in all experiments. The interval prior to the conditioning pulse was 150 and prior to the test pulse, 40 msec. There was little or no recovery from inactivation during the 40 msec between the conditioning and test pulse. In the trace shown, the conditioning pulse voltage was +10 mV. The % inactivation was calculated using the formula: % inactivation = (1 − test pulse current/control pulse current) · 100. (*B*) Peak calcium current elicited by the conditioning pulse (filled symbols) and % inactivation (open symbols) plotted on the same axis as a function of the conditioning pulse voltage. Averaged data from six cells with 3 mM calcium as charge carrier. (*C*) Same as *B*, except 3 mM barium was the charge carrier

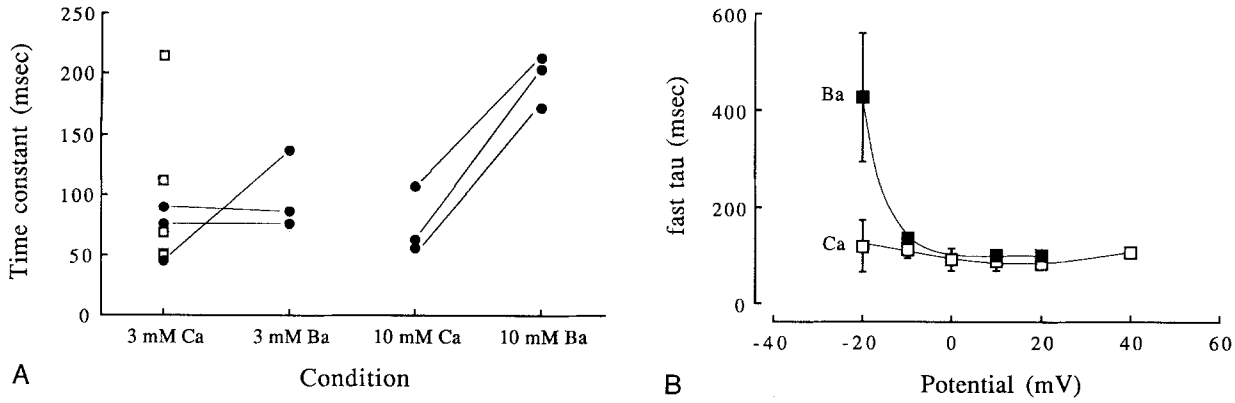

Fig. 3. (*A*) *Left:* Fast time constants, derived from fitting functions as in Fig. 1, are plotted for eight cells in 3 mM calcium (open squares and filled circles), and after replacing calcium with 3 mM barium in three of the cells (filled circles joined by lines). *Right:* Fast time constants in another group of three cells are depicted in 10 mM calcium and after replacing calcium with 10 mM barium. The test potential was 0 mV and the holding potential was −100 mV in each case. (*B*) Fast component time constants plotted as a function of test pulse voltage from a holding potential of −100 mV. Averaged data with 3 mM calcium (open symbols, $n = 7$) or 3 mM barium (filled symbols, $n = 3$)

pulses. In 3 mM calcium (Fig. 2*B*, for six cells), the two curves demonstrated a very similar *U*-shaped voltage-dependence, suggesting that inactivation is due to calcium influx during the conditioning pulse. Maximal inactivation was observed near the peak of the calcium current *I-V* (+10 mV). When this pulse protocol was repeated using 3 mM barium instead of calcium (Fig. 2*C*, for three cells), the degree of inactivation was significantly reduced and less clearly paralleled the *I-V* curve. These findings suggest that fast inactivation was due to the influx of calcium but not barium. Similar results have been reported for other insulin-secreting cells (mouse B-cells: Plant, 1988*b*; HIT cells: Satin & Cook, 1989).

Fast time constants in 3 mM calcium were very variable (Fig. 3*A*), and replacing calcium with equimolar barium-containing solutions produced variable effects, sometimes increasing them (as expected for calcium-influx dependent inactivation) and sometimes not (Fig. 3*A*, left). When 10 mM barium replaced equimolar calcium, however, consistent increases in fast time constants of inactivation were obtained (Fig. 3*A*, right). Since inactivation was not greatly slowed by barium in some cells, suggested voltage may also contribute to fast inactivation. To examine this, fast time constants were measured at different test potentials. As shown in Fig. 3*B*, fast time constants showed little or no voltage dependence in calcium. However, time constants measured in barium were somewhat slower and voltage dependent. The three-pulse and fast time constant data taken together suggests that depolarization as well as calcium influx may contribute to fast inactivation of calcium current.

To determine whether fast inactivation is a characteristic of a low-voltage threshold calcium current component as in HIT cells (Satin & Cook, 1989), we selectively inactivated the fast component with a 300-msec depolarizing prepulse to 0 mV. This produced a 10–20 mV positive shift in the activation threshold obtained following prepulses compared to the control *I-V* curve, and current was significantly reduced at voltages negative to +30 mV (Fig. 4).

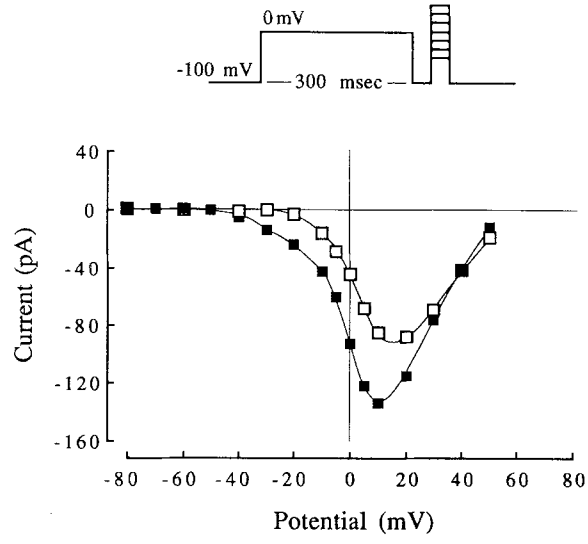

Fig. 4. *Top:* Voltage-clamp protocol used to selectively inactivate the fast current component. *I-V* relations were determined with 40 msec voltage pulses between −120 and +50 mV, with or without a 300 msec prepulse to 0 mV from a holding potential of −100 mV. *Bottom:* Control *I-V* relation (filled symbols) plotted with *I-V* from test pulses preceded by prepulses (open symbols). Data are from one cell in 3 mM calcium

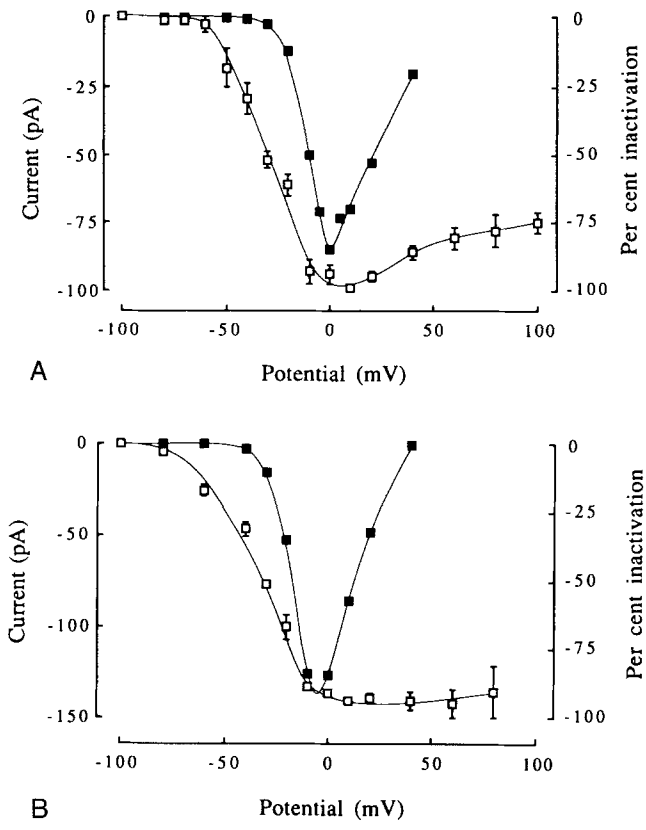

Fig. 5. Inactivation of the slow current component is mediated primarily by voltage. (*A*) Averaged data from six cells in 3 mM calcium using the three-pulse protocol (Fig. 2*A*) except that 10-sec conditioning pulses were used. Peak conditioning pulse current (filled symbols) plotted with % inactivation elicited by the conditioning pulse (open symbols), calculated as in Fig. 2. (*B*) Same as *A*, except averaged data from three cells in 3 mM barium

The near superposition of inward current positive to +30 mV rules out a nonspecific rightward shift of the *I-V* curve. Similar results were obtained in three other cells.

Characteristics of Slowly-Inactivating Component

To establish the mechanism of slow inactivation, 10-sec instead of 100-msec conditioning pulses were used in an otherwise identical three-pulse protocol. Figure 5*A* displays averaged data from six cells, using 3 mM calcium as the charge carrier. In contrast to the results using 100-msec conditioning pulses (Fig. 2*B*), the voltage dependence of the degree of inactivation seen with 10-sec conditioning pulses no longer resembled the peak *I-V* relation: there was substantial inactivation below the calcium current activation threshold (between −40 and −30 mV) as well as at very positive potentials where there was no measurable inward current (> +50 mV). Furthermore, inactivation was greater with prolonged pulses (near 100% between −10 and +10 mV) than with brief pulses (e.g. Fig. 2*B*) with some relief at potentials beyond +10 mV. This may reflect some calcium-dependent inactivation of the fast and/or slow components.

Using 3 mM barium in the same three-pulse protocol would be expected to prevent calcium- but not voltage-dependent inactivation. Figure 5*B* shows the voltage-dependence of inactivation was similar to that obtained with calcium, except that the amount of inactivation in the negative (−60 to −40 mV) and very positive (> +10 mV) voltage ranges was augmented (*see* Discussion). These findings provide additional support that inactivation of the slow component is mediated by voltage.

When 3 or 10 mM calcium was replaced by equimolar barium, the slow time constants usually increased and this was most prominent comparing 10 mM calcium and barium (Fig. 6*A*). However, in both calcium and barium time constants for the slow component were clearly voltage dependent (Fig. 6*B*) and decreased to a relatively constant range of values for increasingly positive voltages. Slow inactivation time constants were insignificantly larger in barium than calcium (Fig. 6*B*). Slow inactivation time constants could not be determined for voltages more negative than −20 mV or positive to +40 mV since the currents were too small. Taken together, the data suggest that while the extent of slow inactivation is primarily mediated by a voltage-dependent mechanism, the rate of inactivation is faster when calcium is charge carrier.

Effects of Holding Potential on Calcium Current

In our studies of neonatal rat and HIT cells, we found that calcium currents had steady-state voltage-dependent inactivation, while results in mouse B-cells suggested the contrary (Plant, 1988*b*). In agreement with our results in the other insulin-secreting cells, we found definite steady-state inactivation at different holding potentials with calcium (Fig. 7*A*) or barium (Fig. 7*B*). The inactivation was reversible and thus unlikely to be due to changes in membrane leakage current, current run-down or irreversible calcium loading.

To test the possibility that fast and slow calcium current components were differentially affected by changes in holding potential as in other systems (Nowycky, Fox & Tsien, 1985; Bean, 1985), current responses elicited by 10-sec voltage pulses from var-

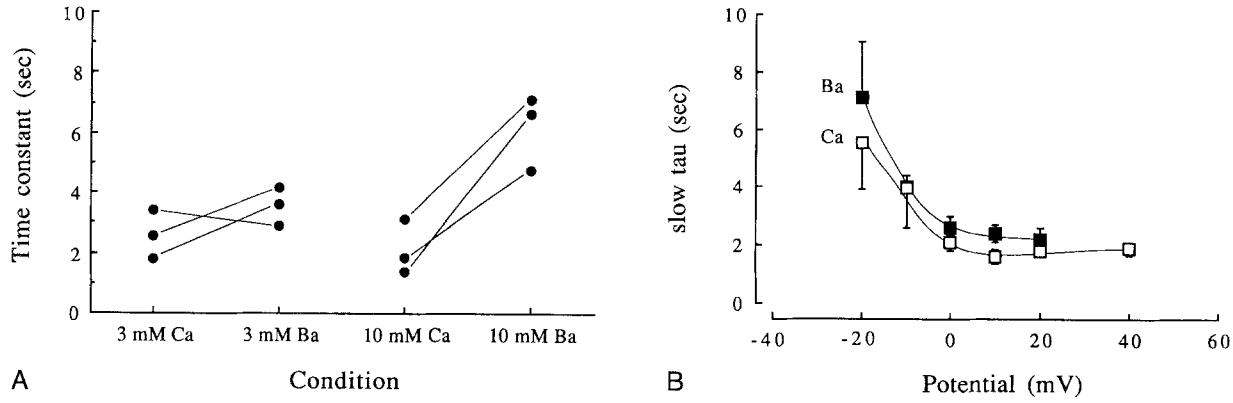

Fig. 6. (*A*) *Left:* Slow time constants plotted for three cells in 3 mM calcium (filled circles), and after replacing calcium with 3 mM barium (lines join data points for each cell). *Right:* Slow time constants in another group of three cells are shown in 10 mM calcium and after replacing calcium with 10 mM barium. (*B*) Slow current component time constants plotted as a function of test pulse voltage from a holding potential of −100 mV. Averaged data with 3 mM calcium (open symbols, $n = 7$) or 3 mM barium (filled symbols, $n = 3$)

ious holding (>30 sec) potentials were compared to those elicited from −100 mV. While the fast component was half-inactivated at about −60 mV, a holding potential of about −40 mV was required to half-inactivate the slow component (Fig. 7*C*). These data suggest that the steady-state inactivation curve for the fast current component is shifted by about 20 mV negative to that of the slow component.

Effects of Barium on the Amplitude of Fast and Slow Current Components

Calcium channel subtypes have been distinguished on the basis of their permeability to barium compared to calcium (Carbone & Lux, 1984; Bean, 1985). To test for this possibility, we compared the current responses to 10-sec voltage pulses to 0 mV elicited in either calcium or barium (10 mM; Fig. 8). The fast component was not appreciably changed when calcium was replaced by barium, while the slow component was increased by a factor of two or more. Although barium can shift the *I-V* relation by about 10 mV negative to that observed in equimolar calcium, these shifts do not account for the selective effect of barium on the slow component amplitude (*data not shown*).

Differential Block by Nimodipine

Since micromolar concentrations of the dihydropyridine calcium channel antagonist nimodipine has been shown to block up to 75% of calcium current in HIT cells (Keahy et al., 1989), we tested whether lower doses might have differential effects on fast and slow current components. Figure 9 displays the effects of 0.5 μM nimodipine on calcium current traces, showing selective suppression of the rapidly inactivating component. Nimodipine blocked 43 ± 4% of the fast calcium current component while having no measurable effect on the slow component during 10-sec voltage pulses to 0 mV from −100 mV. Higher doses (1–10 μM) usually reduced both components (*data not shown*). Assuming that the fast component comprises 36% of total current (Table 1), and assuming nimodipine selectively blocks 43% of the fast component, then about 15% of the peak calcium current should be blocked by nimodipine from a holding potential of −100 mV. This is close to the magnitude of nimodipine block actually observed in a different group of five cells shown in Table 2 (13 ± 2%). Nimodipine (0.5 μM), blocked a larger fraction of calcium current at a holding potential of −40 mV (52 ± 9%) than −100 mV (13 ± 2%; Table 2), possibly reflecting enhanced binding affinity of nimodipine for inactivated calcium channels (Bean, 1984; Sanguinetti & Kass, 1984). The degree of current blockade from a holding potential of −40 mV (52%) was greater than predicted by selective block of fast current based on the data presented in Fig. 7*C* (about 28%). This suggests that the slow current component is subject to voltage-dependent block by nimodipine, since this dose had no effect on the slow component at −100 mV.

Cadmium Sensitivity

Mouse B-cell calcium currents were very sensitive to the calcium channel antagonist cadmium, as expected from previous studies of single calcium chan-

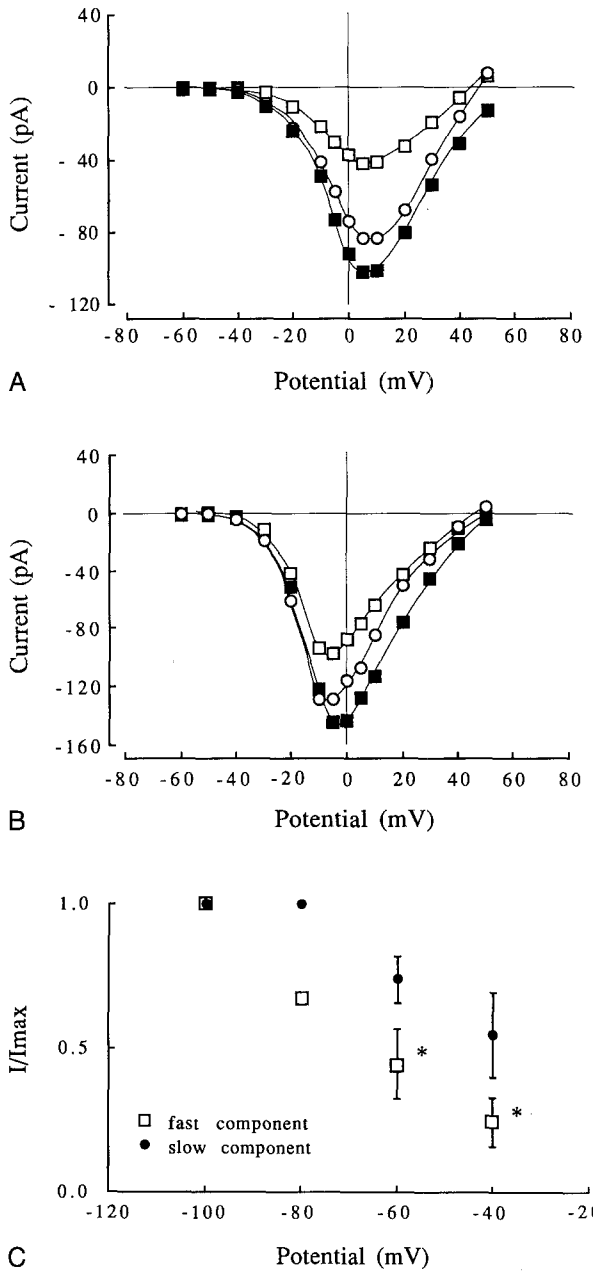

Fig. 7. (*A*) Effect of changes in holding potential on *I-V* relations in 3 mM calcium. *I-V*'s were sampled from holding potentials of −100 mV (filled squares), −60 mV (open circles) and −40 mV (open squares). Averaged data from nine cells. (*B*) Effect of holding potential on *I-V* relations in 3 mM barium. *I-V*'s were obtained from holding potentials of −100 mV (filled squares), −60 mV (open squares) and again from −100 mV (open circles). Averaged data from three cells. (*C*) Differential effects of holding potential on fast and slow calcium current components. I/I_{max} represents the fraction of current activated at holding potentials of −40 mV (n = 6), −60 mV (n = 3) and −80 mV (n = 1) compared to the maximal current elicited at −100 mV. Asterisks signify significant differences in fraction of current activated at −40 and −60 mV between the fast and slow components

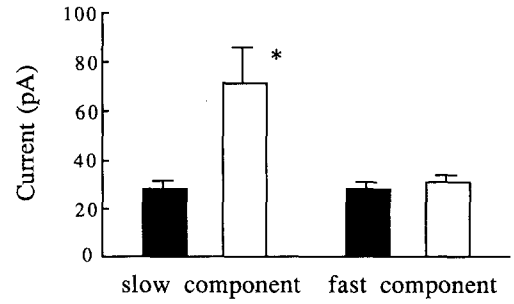

Fig. 8. Differential effect of barium on slow and fast current component amplitudes. The slow and fast component amplitudes in 10 mM calcium (filled bars) and 10 mM barium (open bars) are from the same four cells. The asterisk indicates significant difference in average amplitudes of the slow component between calcium and barium

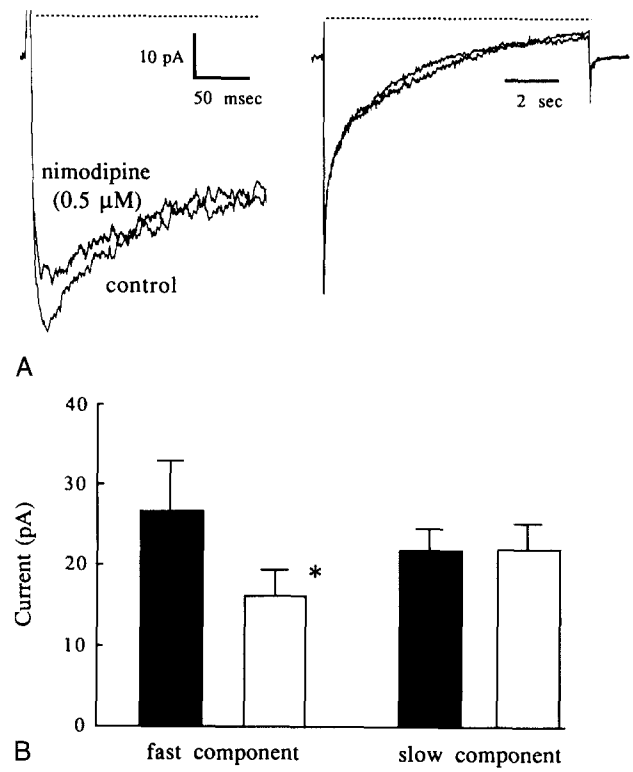

Fig. 9. Effect of nimodipine (0.5 μM) on fast component of calcium current. (*A*) Traces in left panel are the first 200 msec of the current responses elicited by 10-sec voltage pulses to 0 mV from −100 mV shown in their entirety in the right panel. The slow current component in nimodipine is nearly identical to the control trace (right panel), while the fast component amplitude is markedly decreased by nimodipine (left panel). Dashed lines indicate the leak current level in each panel. (*B*) Differential effect of nimodipine on fast and slow current components for three cells. The fast component was reduced by 43 ± 4% in nimodipine (open bars) compared to control (filled bars), but the slow component was not measurably changed. The asterisk indicates significant difference in fast component amplitudes

Table 2. Effect of nimodipine (0.5 μM) on peak calcium current amplitudes (pA) at two different holding potentials (V_h)

	Control (3 mM Ca)	Nimodipine	% Block
Ica (pA) (V_h = −100 mV) (n = 5)	49.7 ± 8.3	43.8 ± 7.6	13 ± 2
Ica (pA) (V_h = −40 mV) (n = 2)	17.6 ± 5.4	9.1 ± 4.3	52 ± 9

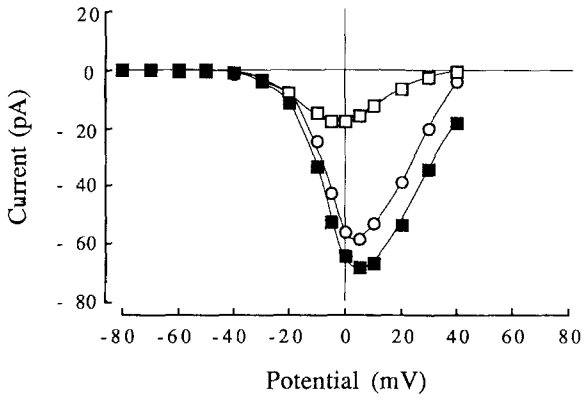

Fig. 10. Effects of cadmium on calcium currents. Control I-V curve (filled squares) plotted with I-V's obtained in 1 μM (open circles) and 10 μM cadmium (open squares). Averaged data from five cells in 3 mM calcium. Inhibition constants (K_i's) were estimated from the data at −20 mV (K_i = 22 μM) and +20 mV (K_i = 2μM) using a single-site binding model for cadmium block of calcium current

nels in these cells (Rorsman et al., 1988) and macroscopic calcium currents in neonatal rat and HIT cells (Satin & Cook, 1988). Figure 10 compares averaged I-V relations from five cells with two doses of cadmium (1 and 10 μM) with the control I-V. The peak of the I-V curve in 10 μM cadmium was shifted by about 10 mV negative to the control curve. The effect of cadmium on calcium current was about tenfold greater at +20 mV (K_i = 2 μM) than at −20 mV (K_i = 22 μM). These results suggest that cadmium preferentially blocked the high-threshold, more slowly-inactivating calcium current component, as previously described in rat and HIT cells (Satin & Cook, 1988).

Discussion

The purpose of this study was to characterize several properties of voltage-dependent calcium currents in cultured adult mouse B-cells. As we have observed in insulin-secreting HIT cells (Satin & Cook, 1989), mouse B-cell calcium currents display two kinetically distinct phases of inactivation in response to 10-sec depolarizing voltage pulses. Nonlinear curve-fitting techniques revealed that the decay of most such currents were adequately fit by the sum of two exponentials, and the time constants differed by over a factor of 30 (Table 1). This approach enabled us to describe the inactivation properties of the fast and slow current components, as well as distinguish these components on the basis of their activation voltage thresholds, steady-state inactivation properties, amplitude when barium was charge carrier, and sensitivity to the calcium channel antagonists nimodipine and cadmium.

Mechanism of Fast Inactivation

We obtained evidence that inactivation of the fast component was mediated by both calcium influx and cell depolarization. Our evidence for a calcium-dependent inactivation mechanism (Brehm & Eckert, 1978; Tillotson, 1979; Eckert & Chad, 1984) is that a conditioning-pulse protocol yielded a U-shaped inactivation-voltage curve which paralleled the peak I-V in calcium, but not in barium. Similar results have been reported in HIT cells (Satin & Cook, 1989) and mouse B-cells (Plant, 1988*b*). However, the maximal amount of calcium-dependent inactivation that we observed in mouse B-cells (27 ± 5%) was less than in HIT cells (45 ± 5%) using the same protocol and experimental conditions.

The degree of inactivation of a subsequent test pulse clearly depended on calcium influx, and the fast time constants of inactivation were markedly slowed when 10 mM calcium was replaced with barium, suggesting that fast inactivation was calcium-dependent. The fast component time constants in 3 mM calcium were highly variable, and replacing calcium with barium did not always slow inactivation (Fig. 3*A*). The time constants of fast inactivation in calcium were not clearly a function of either membrane voltage or calcium current amplitude (Fig. 3*B*). However, the fast component time constants in barium were voltage dependent and, due to the marked variability of the fast time constants in calcium, nearly the same as the average fast time constants in calcium at most voltages (Fig. 3*B*). Additionally, the amplitude of the fast component was dependent on holding potential (*see below*). The data

differ from our previous findings with neonatal rat and HIT cells, where fast inactivation was consistently slowed when calcium was replaced by barium (Satin & Cook, 1989).

Mechanism of Slow Inactivation

Inactivation of the slow current component was mediated by voltage. The inactivation produced by long (10 sec) voltage pulses was prominent below the calcium current threshold (negative to −40 mV) and at very positive potentials where calcium current was not measurable (positive to +50 mV; Fig. 5*A*). When calcium was replaced by barium as charge carrier using this protocol, the voltage-dependence of inactivation was nearly identical, except that the degree of inactivation was augmented by barium (*compare* Fig. 5*A* and *B*). The apparent gradual decrease in inactivation at very positive potentials observed using calcium may reflect calcium-dependent inactivation of the fast and/or slow component. Further support for voltage-dependent inactivation of the slow component can be seen in Fig. 6*B*, where slow time constants decreased with greater depolarization in either calcium or barium.

There are, however, suggestions of an additional calcium dependence to slow inactivation. The data in Fig. 6*A* show that the slow component time constants usually increased when 10 mM calcium was replaced by barium and may have done so in replacing 3 mM calcium. It is paradoxical, then, that the extent of slow inactivation appeared to be actually enhanced when barium was used at both low and high voltages (−50 to −80 mV and at +20 to +50 mV; Fig. 5*A*,*B*). This will require further study. Calcium current components that inactivate via a slow, voltage-dependent mechanism have been described in paramecia (Hennessey & Kung, 1985) and smooth muscle cells (Nakazawa, Saito & Matsuki, 1988).

Effects of Holding Potential on Calcium Currents

I-V relations depended on holding potential between −100 and −40 mV with either calcium or barium as charge carrier (Fig. 7*A*,*B*) as in HIT cells and neonatal rat B-cells (Satin & Cook, 1989). Furthermore, we observed a marked difference in the effect of holding potential on the amount of fast and slow current components available for activation (Fig. 7*C*). From a holding potential of either −60 or −40 mV, a significantly greater fraction of the fast component was inactivated compared to the slow component. These data indicate that the steady-state inactivation curve for the fast component is shifted by about 20 mV negative to that of the slow component. Our results contrast with those of Plant using mouse B-cells (Plant, 1988*b*), who reported no effects of holding potential. We found an effect of holding potential even when using the same pipette solution as used by Plant (*data not shown*).

Evidence Favors Two Calcium Currents in Mouse B-Cells

While it is possible that a single class of calcium channels could explain our findings, we favor the idea that there are at least two calcium channels in mouse B-cells. In addition to a more than 30-fold difference in time constants of inactivation, the two components could be distinguished in a number of ways. The fast component inactivated by both calcium influx- and voltage-dependent mechanisms, showed greater steady-state inactivation at a given holding potential, and a lower voltage threshold than the slow component.The fast component was also more sensitive to block by nimodipine. In contrast, the slow component inactivated primarily by a voltage-dependent mechanism, was increased more than twofold in amplitude when barium replaced calcium as charge carrier (the fast component was not affected) and may have been about 10-fold more sensitive to cadmium than the low-threshold fast component. The data taken together suggest that mouse B-cells possess two calcium currents as we have shown in insulin-secreting HIT cells and neonatal rat B-cells (Satin & Cook, 1988, 1989), although the magnitude of calcium-dependent inactivation of the fast component is clearly different.

Two classes of single calcium channels have been reported in rat (Ashcroft, Kelly & Smith, 1990), insulin-secreting RINm5F cells (Velasco et al., 1988) and human islets (S. Misler, *personal communication*). Other workers have suggested, however, that mouse B-cells have a single class of calcium channel that resembles L-type channels (Rorsman et al., 1988; Smith, Rorsman & Ashcroft, 1989), although both studies reported a second calcium channel on occasion. Detecting a second channel may be difficult for a number of reasons. Single channel conductances for different channels may be identical (Plummer, Logothetis & Hess, 1989); channel openings may be too brief to resolve, particularly in the absence of a calcium channel "agonist" such as Bay K 8644 for L-type channels (Bean, 1989) or channels may be clustered in "hot spots" (Fox, Nowycky & Tsien, 1987*b*; Silver, Lamb & Bolsover 1990) where they would be either missed or in such abundance as to defeat single channel analysis.

Our results do not easily enable us to categorize these calcium current components into the T, N and L nomenclature of calcium channels (Fox, Nowycky & Tsien, 1987*a*; Bean, 1989). The kinetics, steady-state inactivation properties, relative cadmium insensitivity and lack of effect of barium on current amplitude suggest the fast current component to be a T-type current. However, the fast component inactivated via calcium- and voltage-dependent mechanisms and was sensitive to nimodipine, properties not generally associated with this channel type. Recent studies, however, have shown that calcium currents with T-type properties are sensitive to micromolar and submicromolar concentrations of dihydropyridine antagonists in some preparations (Cohen et al., 1988; Akaike, Kostyuk & Osipchuk, 1989). The slowly inactivating component, which has a relatively high voltage threshold, is substantially increased in amplitude in barium, is more sensitive to cadmium block than the fast component and is reduced by micromolar concentrations of nimodipine could correspond to an L-type calcium current. If the fast and slow current components do indeed correspond to T- and L-type calcium currents, respectively, then mouse B-cell calcium currents are similar to rat hypothalamic neurons in having T-type calcium currents that are actually somewhat more sensitive to nimodipine than their L-type calcium current (Akaike et al., 1989).

Possible Physiological Significance of Two Calcium Currents

Both the fast spikes and underlying plateau depolarizations that characterize glucose-induced bursting in B-cells are calcium-dependent action potentials (Dean & Matthews, 1970*b*; Cook, Crill & Porte, 1980; Ribalet & Beigelman, 1980; Meissner & Schmeer, 1981). The fast calcium current component, by virtue of its rapid inactivation kinetics, somewhat lower threshold, and steady-state inactivation properties, may be involved in initiating burst firing and fast action potentials. The slowly inactivating component may underly the sustained plateau depolarizations, typically lasting several seconds. Furthermore, the slow component's recovery from voltage-dependent inactivation during the interburst interval may act in concert with the fast current component to determine the pacing of burst firing. In this manner, the dual regulation of calcium influx by membrane potential and calcium influx itself may serve to provide sufficient calcium to efficiently engage the insulin secretory apparatus of the B-cell without triggering toxic cellular processes that result from sustained elevation of intracellular calcium (Choi, 1988). The possible importance of slow, voltage-dependent inactivation for mouse B-cell bursting electrical activity is underscored by the recent report that intracellular free calcium does not continually accumulate during plateaus in intact mouse islets (Valdeolmillos et al., 1989). Thus, depolarization rather than calcium accumulation may regulate the duration of the plateaus observed in suprathreshold glucose, this in turn may regulate the timing of pulsatile insulin secretion (Rosario, Atwater & Scott, 1986).

We thank Mr. Louis Stamps for cell culturing and other technical assistance. This work was funded by the NIH and the U.S. Veterans Administration.

References

Akaike, N., Kostyuk, P.G., Osipchuk, Y.V. 1989. Dihydropyridine-sensitive low-threshold calcium channels in isolated rat hypothalamic neurones. *J. Physiol.* **412:**181–195

Ashcroft, F.M., Kelly, R.P., Smith, P.A. 1990. Two types of Ca channel in rat pancreatic β-cells. *Pfluegers Arch.* **415:**504–506

Baskin, D.G., Gorray, K.D., Fujimoto, W.Y. 1984. Immunocytochemical identification of cells containing insulin, glucagon, somatostatin and pancreatic polypeptide in the islets of Langerhans of the guinea pig pancreas with light and electron microscopy. *Anat. Rec.* **208:**567–578

Bean, B.P. 1984. Nitrendipine block of cardiac calcium channels: High affinity binding to the inactivated state. *Proc. Natl. Acad. Sci. USA* **81:**6388–6392

Bean, B.P. 1985. Two kinds of calcium channels in canine atrial cells. Differences in kinetics, selectivity, and pharmacology. *J. Gen. Physiol.* **86:**1–30

Bean, B.P. 1989. Classes of calcium channels in vertebrate cells. *Annu. Rev. Physiol.* **51:**367–384

Brehm, P., Eckert, R. 1978. Calcium entry leads to inactivation of calcium channel in *paramecium*. *Science* **202:**1203–1206

Carbone, E., Lux, H.D. 1984.A low voltage-activated, fully inactivating Ca channel in vertebrate sensory neurons. *Nature* **310:**501–502

Choi, D.W. 1988. Calcium-mediated neurotoxicity: Relationship to specific channel types and role in ischemic damage. *Trends Neurosci.* **11:**465–469

Cohen, C.J., McCarthy, R.T., Barrett, P.Q., Rasmussen, H. 1988. Ca channels in adrenal glomerulosa cells: K^+ and angiotensin II increase T-type Ca channel current. *Proc. Natl. Acad. Sci. USA* **85:**2412–2416

Cook, D.L., Crill, W.E., Porte, D., Jr. 1980. Plateau potentials in pancreatic islet cells are voltage-dependent action potentials. *Nature* **286:**404–406

Cook, D.L., Hales, C.N. 1984.Intracellular ATP directly blocks K^+ channels in pancreatic islet cells. *Nature* **311:**271–273

Dean, P.M., Matthews, E.K. 1970*a*. Glucose-induced electrical activity in pancreatic islet cells. *J. Physiol.* **210:**255–264

Dean, P.M., Matthews, E.K. 1970*b*. Electrical activity in pancreatic islet cells: Effect of ions. *J. Physiol.* **210:**265–275

Eckert, R., Chad, J.E. 1984. Inactivation of Ca Channels. *Prog. Biophys. Molec. Biol.* **44:**215–267

Fabiato, A., Fabiato, F. 1979. Calculator programs for computing the composition of the solutions containing multiple metals and ligands used for experiments in skinned muscle cells. *J. Physiol. (Paris)* **75:**463–505

Findlay, I., Dunne, M.J. 1985. Voltage-activated Ca^{2+} currents in insulin-secreting cells. *FEBS Lett.* **189:**281–285

Fox, A.P., Nowycky, M.C., Tsien, R.W. 1987*a*. Kinetic and pharmacological properties distinguishing three types of calcium currents in chick sensory neurones. *J. Physiol.* **394:**149–172

Fox, A.P., Nowycky, M.C., Tsien, R.W. 1987*b*. Single-channel recordings of three types of calcium channels in chick sensory neurones. *J. Physiol.* **394:**173–200

Hamill, O.P., Marty, A., Neher, E., Sakmann, B., Sigworth, F.J. 1981. Improved patch clamp techniques for high-resolution current recording from cells and cell-free membrane patches. *Pfluegers Arch.* **391:**85–100

Hennessey, T.M., Kung, C. 1985. Slow inactivation of the calcium current of *paramecium* is dependent on voltage and not internal calcium. *J. Physiol.* **365:**165–179

Hille, B. 1984. Ionic channels of excitable membranes. Sinauer Associates, Sunderland (MA)

Hiriart, M., Matteson, D.R. 1988. Na channels and two types of Ca channels in rat pancreatic B cells identified with the reverse hemolytic plaque assay. *J. Gen. Physiol.* **91:**617–639

Hopkins, W.F., Satin, L.S., Cook, D.L. 1989. Calcium and depolarization-dependent Ca current inactivation in cultured mouse B-cells. *Diabetes* **38(Suppl. 2):**96A

Keahy, H., Rajan, A.S., Boyd, A.E., III, Kunze, D.L. 1989. Characterization of voltage-dependent Ca^{2+} channels in β-cell line. *Diabetes* **38:**188–193

Meissner, H.P., Schmeer, W. 1981. The significance of calcium ions for the glucose-induced electrical activity of pancreatic B cells. *In:* The Mechanism of Gated Calcium Transport Across Biological Membranes. S. Ohnishi and M. Endo, editors. pp. 157–165. Academic, New York

Meissner, H.P., Schmelz, H. 1974. Membrane potential of B-cells in pancreatic islets. *Pfluegers Arch.* **351:**195–206

Nakazawa, K. Saito, H., Matsuki, N. 1988. Fast and slowly inactivating components of Ca-channel currents and their sensitivities to nicardipine in isolated smooth muscle cells from rat vas deferens. *Pfluegers Arch.* **411:**289–295

Nowycky, M., Fox, A.P., Tsien, R.W. 1985. Three types of neuronal calcium channels with different agonist sensitivity. *Nature* **316:**440–443

Plant, T.D. 1988*a*. Na^+ currents in cultured mouse pancreatic B-cells. *Pfluegers Arch.* **411:**429–435

Plant, T.D. 1988*b*. Properties and calcium-dependent inactivation of calcium currents in cultured mouse pancreatic B-cells. *J. Physiol.* **404:**731–747

Plummer, M.R., Logothetis, D.E., Hess, P. 1989. Elementary properties and pharmacological sensitivities of calcium channels in mammalian neurons. *Neuron* **2:**1453–1463

Ribalet, B., Beigelman, P.M. 1980. Calcium action potentials and potassium permeability activation in pancreatic B-cells. *Am. J. Physiol.* **239:**C124–C133

Rorsman, P., Ashcroft, F.M., Trube, G. 1988. Single Ca channel currents in mouse pancreatic B-cells. *Pfluegers Arch.* **412:**597–603

Rorsman, P., Trube, G. 1986. Calcium and delayed potassium currents in mouse pancreatic β-cells under voltage-clamp conditions. *J. Physiol.* **374:**531–550

Rosario, L.M., Atwater, I., Scott, A.M. 1986. Pulsatile insulin release and electrical activity from single ob/ob mouse islets of Langerhans. *In:* Biophysics of the Pancreatic B-Cell. I. Atwater, E. Rojas, and B. Soria, editors. pp. 413–425. Plenum, New York

Sanguinetti, M.C., Kass, R.S. 1984. Voltage-dependent block of calcium channel current in calf cardiac purkinje fiber by dihydropyridine calcium channel antagonists. *Circ. Res.* **55:**336–348

Satin, L.S., Cook, D.L. 1985. Voltage-gated Ca^{2+} current in pancreatic B-cells. *Pfluegers Arch.* **404:**385–387

Satin, L.S., Cook, D.L. 1988. Evidence for two calcium currents in insulin-secreting cells. *Pfluegers Arch.* **411:**401–409

Satin, L.S., Cook, D.L. 1989. Calcium current inactivation in insulin-secreting cells is mediated by calcium influx and membrane depolarization. *Pfluegers Arch.* **414:**1–10

Satin, L.S., Hopkins, W.F., Fatherazi, S., Cook, D.L. 1989. Expression of a rapid, low-voltage threshold K^+ current in insulin-secreting cells is dependent on intracellular calcium buffering. *J. Membrane Biol.* **112:**213–222

Silver, R.A., Lamb, A.G., Bolsover, S.R. 1990. Calcium hotspots caused by L-channel clustering promote morphological changes in neuronal growth cones. *Nature* **343:**751–754

Smith, P.A., Rorsman, P., Ashcroft, F.M. 1989. Modulation of dihydropyridine-sensitive Ca^{2+} channels by glucose metabolism in mouse pancreatic B-cells. *Nature* **342:**550–553

Tillotson, D. 1979. Inactivation of Ca conductance dependent on entry of Ca ions in molluscan neurons. *Proc. Natl. Acad. Sci. USA* **76:**1499–1500

Valdeolmillos, M., Santos, R.M., Contreras, D., Soria, B., Rosario, L.M. 1989. Glucose-induced oscillations of intracellular Ca^{2+} concentration resembling bursting electrical activity in single mouse islets of Langerhans. *FEBS Lett.* **259:**19–23

Velasco, J.M. 1987. Calcium channels in rat insulin-secreting RINm5F cell line. *J. Physiol.* **398:**15P

Velasco, J.M., Petersen, J.U.H., Petersen, O.H. 1988. Single-channel Ba^{2+} currents in insulin-secreting cells are activated by glyceraldehyde stimulation. *FEBS Lett.* **231:**366–370

Wollheim, C.B., Pozzan, T. 1984. Correlation between cytosolic free Ca^{2+} and insulin release in an insulin-secreting cell line. *J. Biol. Chem.* **259:**2262–2267

Wollheim, C.B., Sharp, W.G. 1981. Regulation of insulin release by calcium. *Physiol. Rev.* **61:**914–973

Received 18 April 1990; revised 24 July 1990